Research Paper

The Holocene
1–14

DOI: 10.1177/09596836231176501
journals.sagepub.com/home/hol
Sage

Holocene geomorphological and pedosedimentary archives of eastern Sahelian paleoenvironments (Kassala, Sudan)

Stefano Costanzo,[1] Andrea Zerboni[2] and Andrea Manzo[1]

Abstract

Studies upon past climates, natural landscapes, and environments of archaeologically pivotal regions of northern Africa have been of paramount interest in the past decades. For some of those regions, the human-environmental nexus, intended as the biunivocal mutual agency between people and nature, has been a long-standing research question; yet, for other areas, the environmental record is a still unexplored archive. Here we present case studies discussing archaeo-environmental sites from the easternmost stretches of the Sahelian belt, in the Kassala region of Sudan. Therein, in a landscape that is currently characterized by granitoid rocky outcrops dotting a vast gravelly pediplain colonized by xerophytes and thin ephemeral grass, pedosedimentary features that encase the climatic history of the region are found. By means of field survey, physico-chemical laboratory analyses, micromorphological analyses, and radiometric dating, we investigated the uppermost portion of the Quaternary record to contextualize the Late-Holocene archaeological record. The main identified features include buried isohumic soil horizons in lower flat grounds, which are legacy of water-reliant prairie environments formed in the wetter Early to Middle Holocene, and later accretional dusty aeolian deposits intermingled with colluvial gravels close to the outcrops' eroded foothills, testimony of a climatic deterioration towards aridity and erosion driven by hyper seasonality. Results are of great importance as a contribution to a more holistic understanding of past human economies of the region, as well as being a newly added tile to the reconstruction of surface processes dynamics over Africa and their response to global climate changes.

Keywords

desert loess, Holocene, isohumic soil, paleoenvironment, Sahel, Sudan

Received 21 January 2023; revised manuscript accepted 4 April 2023

Introduction

Studies upon the reconstruction of the paleoenvironmental settings of African deserts and their margins have a long-standing tradition shared by archaeologists, geoscientists and ecologists in the broadest sense, stemming from the necessity of understanding the evolution of the natural world where past societies rose, thrived and fell (e.g. Brass, 2018; Clarke et al., 2016; Gasse, 2000; Gatto and Zerboni, 2015; López-García et al., 2013; Mercuri et al., 2022; Nicoll, 2004; Ritchie and Haynes, 1987). In arid lands, scholars documented the occurrence, within in the geological record, of pedosedimentary features that are incompatible with present-day dryland climates and environs (Cremaschi et al., 2010; Nicoll et al., 2021). Because such natural contexts were often found intimately mixed with archaeological remains, it quickly became clear that the very nature of human settlements, migrations and achievements throughout the archaeological past needed to be – at least partially – scrutinized through the lens of physical geography and environmental changes (Butzer, 1982; Heitz et al., 2021). Under this scope, the Sahara and Sahel received the scrutiny of several generations of archaeologists and scientists looking to decipher the remarkable diversity of their environmental and cultural contexts *sensu latu* (some examples on the Nile Valley: Butzer, 1959, 1960, 1980; Caton-Thompson and Gardner, 1932; Sandford, 1929), possibly driven by an inherited condition derived from the long-standing antiquarian tradition born from the explorations of the Nile Valley and the Mediterranean coast of Africa (Manzo, 2017).

Of all periods identified within the geological and pedostratigraphic record, the Holocene is the best characterized. Features and proxies formed during the Holocene are usually found in accessible settings close to surface in sedimentary sequences or even directly exposed in subaerial environments, and although they are often fragmentary because of past and extant erosional processes (Swezey, 2001), they are generally better preserved and provide a higher resolution compared with older features. Over time, this allowed for the build-up of extremely detailed environmental characterizations of small and large areas, with highly-resolved temporal anchorages. Results contributed to define, on a supra-regional scale, a succession of former Holocene climates and environments; most notably, in Northern Africa two major trends happened after

[1]Dipartimento Asia, Africa e Mediterraneo, Università degli Studi di Napoli 'L'Orientale', Italy
[2]Dipartimento di Scienze delle Terra 'A. Desio', Università degli Studi di Milano, Italy

Corresponding author:
Stefano Costanzo, Dipartimento Asia, Africa e Mediterraneo, Università degli Studi di Napoli 'L'Orientale', Piazza San Domenico Maggiore 12, Napoli 80134, Italy.
Email: ste.costanzo92@gmail.com

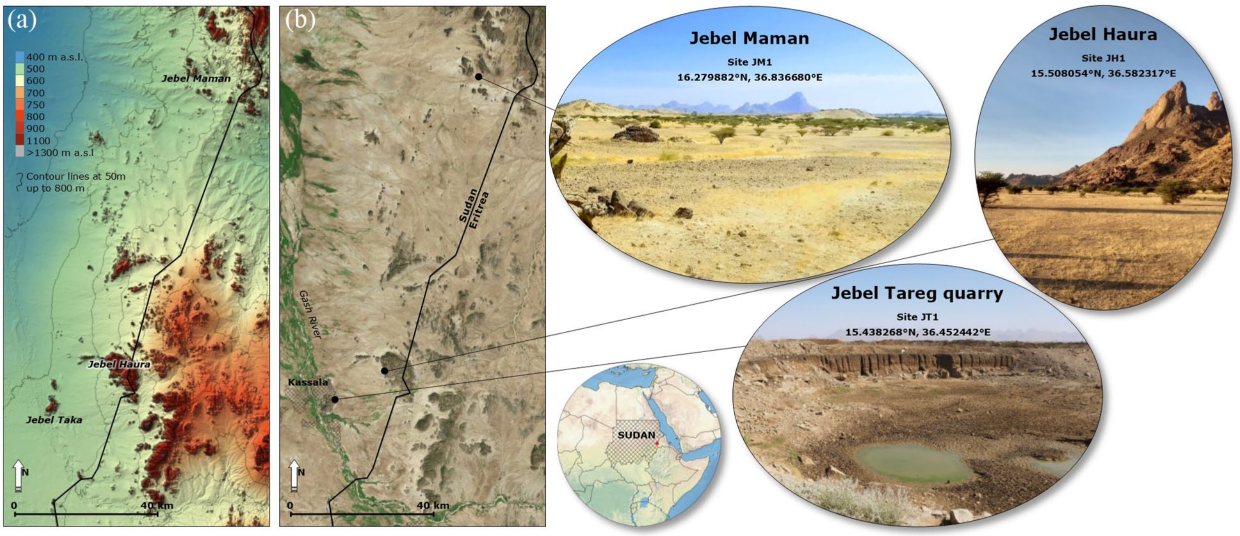

Figure 1. Overview of the study region and each investigated site. (a) Digital Elevation Model (DEM) of the area, highlighting the regional topography characterized by steep rocky inselbergs emerging from a vast pediplain and alluvial plain. (b) Satellite overview of the area, highlighting the locations of investigated sites JM1, JH1, and JT1 (round panels).

the end of the Last Glacial Maximum (Gasse, 2000; Gatto and Zerboni, 2015): the so-called African Humid Period (AHP) (~11000–5000 BP) (DeMenocal and Tierney, 2012), dotted by several Rapid Climatic Events (RCCs) (Mayewski et al., 2004), and the following process of aridification that is still ongoing in the present-day (Cremaschi et al., 2014; Jaouadi et al., 2016). The former is the latest period in the Saharan climatic history characterized by enhanced water availability compared to today, which contributed to the sustenance of riverine and lacustrine habitats well within the continent's interior (Bristow et al., 2018; Cremaschi et al., 2010). The latter period, still debated regarding its onset (Shanahan et al., 2015) and variable regional impact upon the human peopling and migrations from marginal areas towards large surviving rivers (Gatto and Zerboni, 2015; Wright, 2017; Zerboni and Nicoll, 2019), is characterized by a downfall in annual rainfall yield that is, however, mitigated by hyperseasonal precipitations especially along the Sahelian belt (Costanzo et al., 2022; Hulme and Tosdevin, 1989; Zhang et al., 2012).

The aim of this work is to provide kickstarting data on the Holocene climatic and environmental evolution of the portion of the Kassala region of Sudan laying east of the Gash River (Figure 1), a drastically understudied geographical area, to frame and contextualize it within the wider – and better represented – supra-regional picture. By means of field survey, sedimentological analyses, micromorphological analyses and radiometric dating, we present the results for three sites spread over an area extending from the outskirts of the city of Kassala to the southern stretches of the Sudanese Red Sea Hills (Figure 1). All sites are located close to the foothill of imposing rocky outcrops, where complex palimpsests of aeolian, colluvial, and hydric landforms, intertwined with paedological bodies, encapsulate the paleoenvironmental history of the region and, occasionally, host rich archaeological remains. Results place the sites within the known supra-regional Holocene climatic history of Saharan and Sahelian Africa, with found evidence of fossil grasslands from the AHP, as well as intricate polygenic aeolian-colluvial deposits from the arid/hyperseasonal later and recent periods.

Physiography and archaeology of the region of Kassala

The region of Kassala is an administrative division of the far Eastern Sudan, a sparsely inhabited territory of the far eastern Sahelian belt with a hot semi-arid (BSh) to hot desert (BWh) climate (Beck et al., 2018), separated into two physiographic sub-regions by the present-day S-N course of the Gash River. To the west, the vast agricultural alluvial plain of the Southern Atbai extends from the Gash River up to the Atbara River and beyond, merging into Central Sudan's Butana Plain and eventually reaching the Nile. To the east, a vast, gently sloping pediplain connects the alluvial plains with the western edge of the Eritrean Highlands and the southern periphery of the Red Sea Hills (Costanzo et al., 2021a). The pediplain is the late-stage result of dismantling cycles of the crystalline basement and emerged plutons that compose the Proterozoic orogenic complex of the Arabian Nubian Shield (Costanzo et al., 2021a; Johnson et al., 2011). The extant landscape is characterized by hundreds of gneissic and granodioritic inselbergs (called *jebels*, Arabic for mountains) emerging from the gravelly surface in the form of whaleback rocks and imposing bornhardt assemblages. Inselbergs often have jagged perimeters, which create spurs and secluded valleys that over time became relatively protected niches where the archaeological, pedostratigraphic and geomorphological records are better preserved in comparison with the open plains, such is the case, for example, of the valley of Mahal Teglinos (Costanzo et al., 2022; Swezey, 2001). An intricate drainage network originates from the inselbergs: precipitation is gathered on the rocky outcrops following radial or rectangular patterns, depending on the dimension of each outcrop and the incidence and morphology of faults and joints within the rock. Water converges downslope into large dendritic systems, which then merge into medium-sized braided channels flowing towards the lower plains and ultimately splitting into splays and sheet flows on increasingly flatter ground down to the Gash River (Costanzo et al., 2021a). The extant drainage system is fed by seasonal rainfall, which, paired with the steep gradient of the inselbergs' hillsides, causes flash floods that consistently erode and mobilize the Late Quaternary unconsolidated deposits constituting the coalescing pediments encircling each outcrop, resulting in the formation of deep and pervasive badlands. Therein, gullying is a geomorphological threat for people, livestock, and the archaeological and environmental records alike (Costanzo et al., 2022).

Archaeological research in the region shed light on human occupation dating from the Palaeolithic (Abbate et al., 2010; Nassr, 2014; Shiner, 1971) up to sub-recent periods, with the settlement of hunting-foraging communities during the Early/Middle Holocene (Amm Adam, Malawiya Groups), and a great flourishing of civilizations especially during the Middle/Late-Holocene, which saw the world's first domestication of *Sorghum* sp. (Butana Group) (Beldados et al., 2018; Winchell et al., 2017) and the emergence of well-structured societies (Gash, Mokram, Hagiz, Khatmiya, Gergaf Groups), who took active part to commercial trades and routes between the Nile Valley and the Horn of Africa and Arabian Peninsula (Fattovich et al., 1988; Manzo, 2017 and references therein; Manzo, 2020). Nevertheless, due to general logistic convenience and the presence of more glaring and easily explorable sites, archaeological research focused primarily on the Gash river's alluvial plain and the valley of Mahal Teglinos, which is located just outside the city of Kassala, a few hundred meters east of the river (Manzo, 2017). For this reason, the strip of land comprised between the Gash and the Sudanese-Eritrean border, which amounts to roughly 5000 km^2, is still mostly unexplored both from an archaeological and paleoenvironmental point of view. Nonetheless, a few published works upon the late Medieval Islamic funerary monuments scattered in the landscape (Costanzo et al., 2021b; Crowfoot, 1922; Elsadig, 2000; Paul, 1952) and a newly identified relevant Gash Group site located at the foothill of a large rocky outcrops (Giancristofaro, 2021) are starting to define the effective archaeological potential and value of the region.

Methods

Field survey

Field survey was planned upon desk-based visual inspection of free satellite imagery (GoogleEarth™) and available published regional geomorphological and geological cartography (Costanzo et al., 2021a; Geological Research Authority of the Sudan [GRAS], 2004), in order to identify locations of high archaeological-environmental potential yet easily reachable with ordinary vehicles and trekking equipment. On location, field walks and surface finds collections were executed, recording each notable find with a GPS tracker. Three most notable locations were chosen as exemplary for this work: a gully exposing a newly identified Gash Group site (Giancristofaro, 2021) at the western foothill of Jebel Haura (Site JH1), the gneiss quarry of Jebel Tareg (Site JT1) and the rill-carved pediments of the Jebel Maman hills complex (Site JM1) (Figure 1).

Pedosedimentological and micromorphological analyses

Sedimentological analyses were carried out on bulk soil samples collected from the sections that were identified during the field surveys and selected for their potential information yield, such as the presence of diverse pedostratigraphic features and archaeological material and layers. When possible, preliminary assessments of the depositional and erosional processes were defined based on the sediment's texture and structure, and chronologies were defined based on archaeological material found therein. Samples were collected from bottom to top to avoid contamination from each layer/horizon – when identifiable – or at regular intervals of 15 cm, as in the case of the 4 m section of Jebel Haura. The samples were stored in plastic bags and labelled accordingly.

Physical and chemical laboratory characterization of sediments included the following analyses: (i) grain-size distribution, performed after removing organics by hydrogen peroxide (130 vol) pre-treatment; sediments were wet sieved (diameter 1.0–0.63 mm), then the fine fraction (<0.63 mm) was determined by hydrometer based on Stokes' law (Gale and Hoare, 2012); (ii) loss on ignition (LoI), used as a proxy for the evaluation of the total organic carbon content (Heiri et al., 2001) and (iii) humified organic carbon matter, performed measuring the oxidizable organic carbon through titration after chromic acid treatment (Walkley and Black, 1934); (iv) calcium carbonate equivalents, estimated from the CO_2 emitted by the sample after reacting with HCl with the Dietrich–Frühling calcimeter (Gale and Hoare, 2012).

Thin sections for micromorphology (45 mm × 85 mm mounted on a glass support) were manufactured from oriented and undisturbed sediment blocks by Massimo Sbrana 'Servizi per la Geologia' laboratory (Piombino, Italy – serviziperlageologia.it). The preparation followed the procedure described by Murphy (1986). The thin sections were studied employing an optical petrographic microscope (Olympus BX41) mounting a digital camera (Olympus E420) for the acquisition of high-quality images. Observation was carried out at various magnifications (20×, 40×, 100×, 400×) under plane polarized light (PPL) and cross-polarized light (XPL). The description of the thin sections followed the terminology suggested by Stoops (2021), and their interpretation was aided by the coloured atlases and concepts summarized in Nicosia and Stoops (2017), Macphail and Goldberg (2018), and Stoops et al. (2018).

Radiocarbon dating

Radiocarbon dating was carried out to anchor pedostratigraphies to absolute chronologies. Due to the marked morphogenetic dynamism of the interspersed archaeological and natural deposits, which are often tainted by post-depositional displacement and therefore prone to stratigraphic misinterpretation (Costanzo et al., 2022), single fragments of organic remains were avoided, favouring the collection of bulks of organic-rich soil samples from extensive layers in primary deposition instead. Radiocarbon dates were calibrated using the software OxCal 4.4, with the calibration curve IntCal20 (Reimer, 2020). A total of two bulks of organic-rich soil, one for Site JT1 and one for Site JM1 (see below), were destined for radiocarbon dating.

Results

Jebel Haura – Site JH1

Jebel Haura is a large inselberg composed of steep granodioritic bornhardts, located 20 km east of the city of Kassala (Figure 1). Its highest peaks reach ~1200 m a.s.l., with a prominence of ~650 m. Slopes at high altitudes are either bare rock etchplains or covered with stabilized gravelly debris. At lower altitudes, a chaos of boulders and coalescing gravelly taluses accumulate and gradually intertwine with the foothill pediment matching its gradient (Figure 2a). At the very outskirts of the pediment, a deeply weathered paleosoil, likely related to pre-Pleistocene warm and humid climatic phases, is found underlying the Holocene sequence. The pediment is composed of interlayered, very fine to coarse unconsolidated sediments. A general in-situ understanding of its sedimentological features was made possible by the widespread occurrence of large gullies (Figure 2a and b), which scar the deposit with retreating vertical cliffs reaching heights of 4–6 m, exposing sections that disclose the geomorphological palimpsest. The examined section (Figure 2c) was chosen considering cliff stability, that is, absence of undercuts or overhangs, accessibility and presumed information yield. The section is 4 m high, and reveals two main sedimentary units: (i) a ~1.5 m thick sand-dominated deposit characterized by faint cross- and planar-beddings, likely created by chaotic high-energy water runoff, superimposed with (ii) a 2.5 m thick dust-dominated deposit characterized by a generally massive structure, enriched with coarse sand and gravel and interspersed with lenses of gravelly colluvium containing rich protohistoric archaeological layers (Figure 2d).

Results from the pedosedimentological analyses substantiate the field observations. Grain size distribution (Figure 2d) show sand-dominated sediments throughout the deposit, but a closer

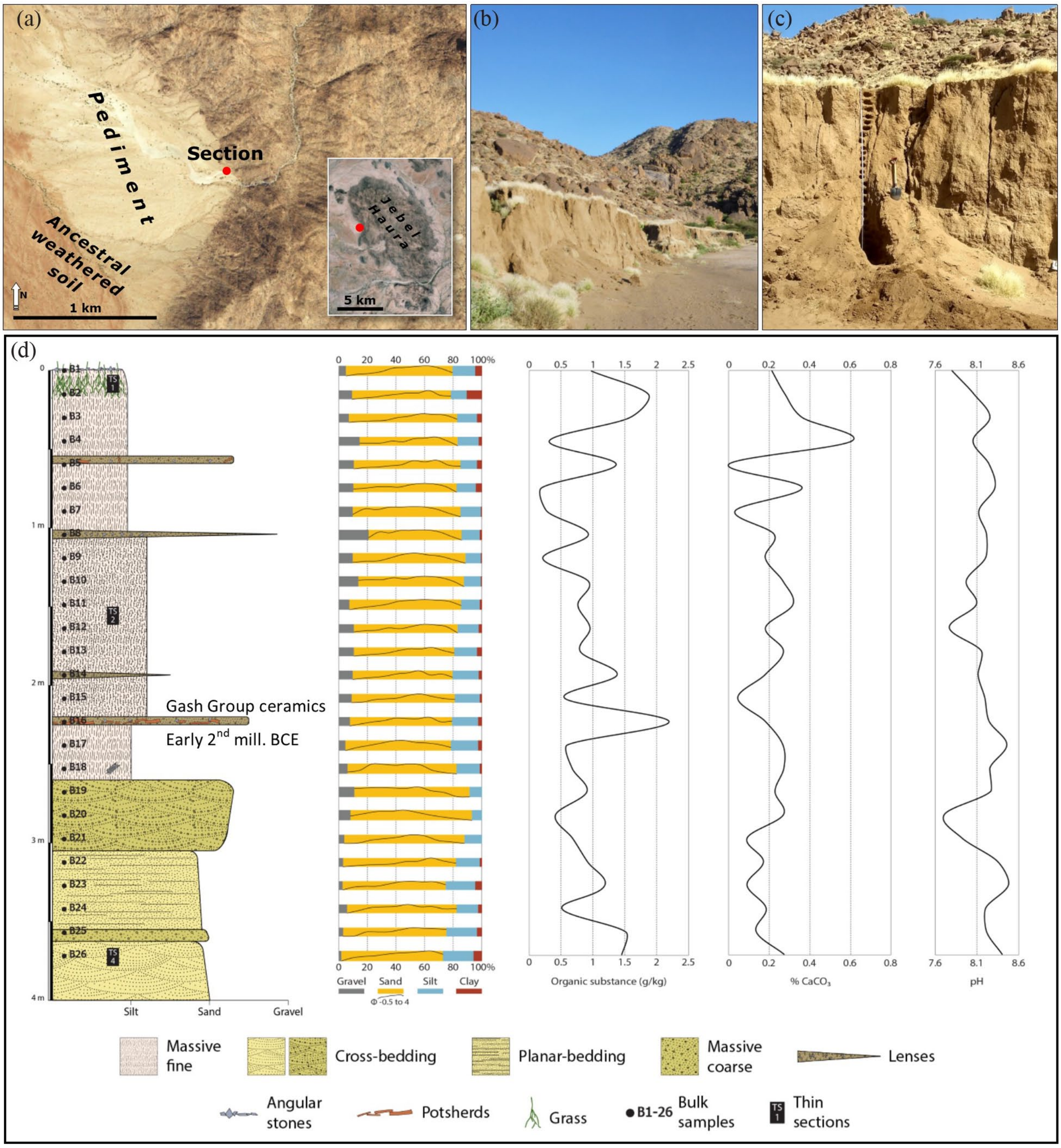

Figure 2. Jebel Haura – Site JH1. (a) Satellite view (GoogleEarth©) of the area. The unconsolidated sandy silty pediment thins out westwards, covering the ancestral laterites. (b) East-facing panoramic view of the gully-exposed section selected for the analyses. The rocky hills in the background are part of the granodioritic bornhardt assemblage of Jebel Haura. The headwaters of the eroding gully are gathered within the valleys found between the bornhardts. (c) The examined portion of the section (15.508054°N, 36.582317°E), measuring 4 m. Shovel left for scale. (d) Results of the pedosedimentary analyses carried out on the bulk samples gathered from the section. From left to right: stratigraphic log with samples and main archaeological features, cumulative grain size distribution, organic substance content, $CaCO_3$ content, pH.

examination on the nuances of the coarser and finer fractions is diagnostic of different morphogenetic processes underlying the formation of the two main units. The lower portion of the deposit (samples B26 – B19 in Figure 2d) is characterized by poor sediment sorting, with large amounts of medium-sized sand but relatively abundant silt and clay as well, identifiable in thin section micromorphology (JH1 TS4, Figure 2d) as a ubiquitous fibrous and powdery coating of all aeolian and colluvial quartz and granodioritic grains, which are loosely arranged in a pellicular grain/spongy microstructure with a chitonic to close porphyric C/F related distribution and faintly layered structure (Supplemental Materials 1 and Figure 3b and c). Samples B20 and B19, in particular, are enriched with gravel and coarse sand, consistent with the turbulent foothill water-lain strata geometry observed on field. Samples B18 to B1, conversely, show an overall prevalence of finer sand, silt and clay, although a general poor sediment sorting and a significant fraction of gravel is present throughout. Particularly, gravel-enriched extensive strata and lenses are recurrent (samples B16, B14, B8, and B5), and two of these (samples B16 and B5) also encase significant amounts of archaeological material, which in a portion of the section located a few tens of metres closer to the foothill is so abundant that it can be safely considered a large, still yet-to-be-explored archaeological site (Giancristofaro, 2021). The analysis of total organic carbon, and that of $CaCO_3$ content also provide meaningful result upon the formation processes of the deposit. Carbon content peaks, in fact, fit

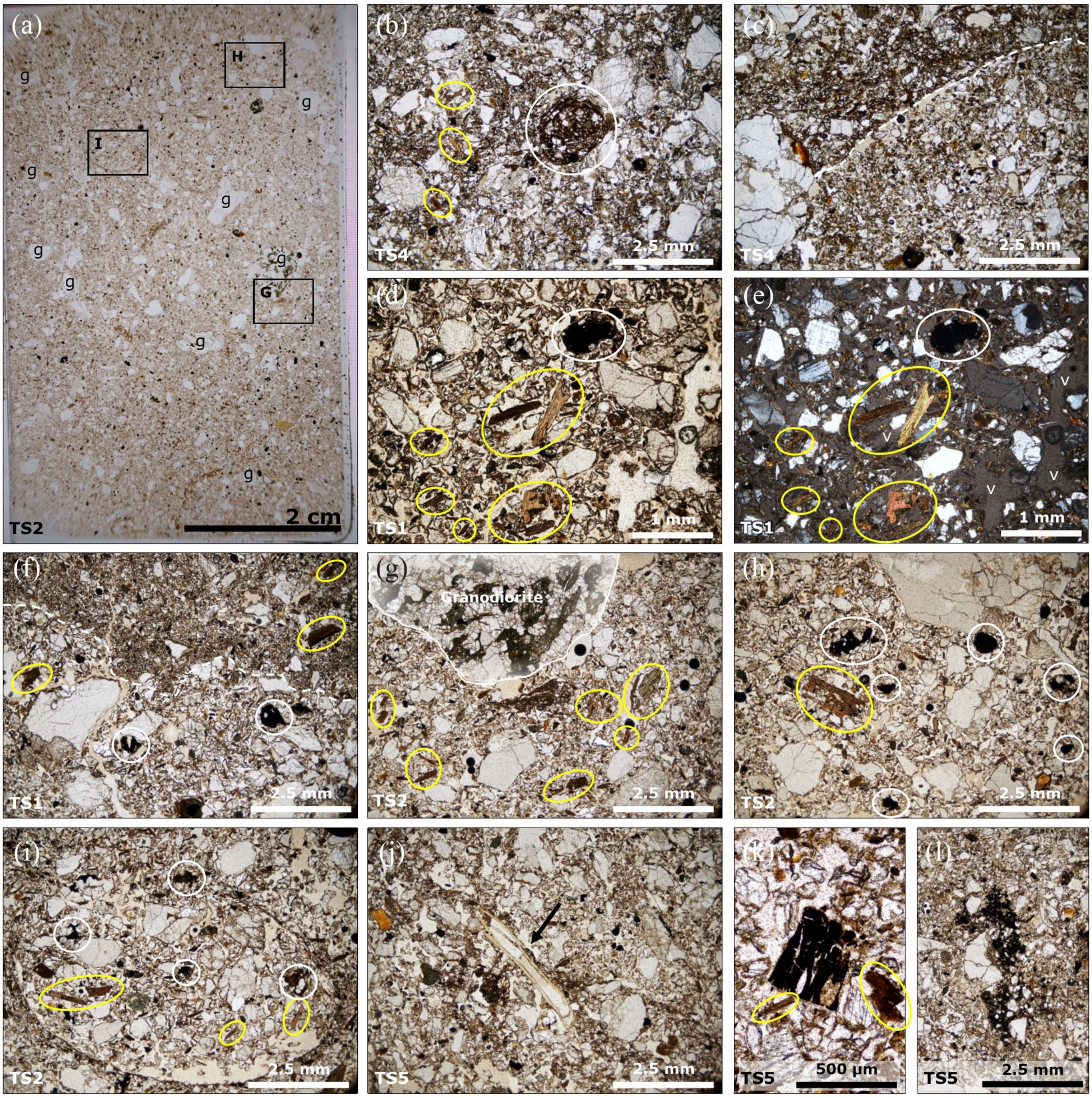

Figure 3. Selected thin section micrographs from Site JH1. (a) Scan of sample JH19TS2, representative of the general appearance of the other samples as well. The boxes refer to panels G, H and I. A few gravel-sized granitoid clasts are indicated with (g). (b and c) PPL micrographs of sample TS4. Gravel-sized quartz, granitoid clasts and rolled pedorelicts (white circle) are visible within the background mass of faintly layered aeolian quartz fine sand coated with fibrous groundmass, sporadically compressed and enriched with dark humic matter (top half in (c)). Yellow circles indicate biotite flakes (d and e) PPL and XPL micrographs of TS1. Gravel- and loess-sized quartz clasts, coated with fibrous groundmass, are visible throughout, and large structural voids (v, dull grey areas in XPL) are visible between grains and aggregates. Swelling biotite flakes (yellow circles) and magnetite fragments (white circles) are also commonly found. (f) Layered zonation between fine-humic (above dashed line) and coarse-sterile (below dashed line) sediment in TS1, with biotite (yellow circles) and magnetite (white circles) visible together among dominant quartz clasts. (g and h) PPL micrographs of TS2 showing very large granodioritic and granite clasts at the top left and top right corners respectively, included within aeolian quartz fine sand coated with fibrous groundmass. Swelling biotite flakes (yellow circles) and magnetite fragments (white circles) are also visible. (i) PPL micrographs of a large bioturbation channel in TS2, backfilled with mineral grains from the collapsed roof. Biotite flakes (yellow circles) and magnetite fragments (white circles) are visible. (j–l) PPL micrographs of TS5, showing organic inclusions such as a bone fragment (black arrow in (j)), a small charcoal fleck (k) (biotite in yellow circles), and a localized soot patch (l).

positively with the gravel-bearing lenses and layers, with greater concentrations in correspondence with the richer archaeological strata and close to the upper surface of the deposit, where live grass roots taint the results. Conversely, $CaCO_3$ concentration peaks fits negatively against the organic carbon, suggesting the existence of periods of environmental stasis associated with intensive human frequentation alternating with periods of aeolian deposition associated with temporary abandonment. Micromorphology of samples JH1 TS2 and JH1 TS1 (Supplemental Materials), taken in correspondence with low-carbon/high $CaCO_3$ layers, yields result consistent with the sedimentological analyses, showing chaotic loose assemblages of dominant aeolian quartz sand and swelling biotite flakes interspersed and faintly layered with hornblende and magnetite-rich granodioritic gravel. All mineral grains are coated with fibrous and powdery micrite, and are arranged in pellicular grain microstructures with chitonic C/F related distribution, with very scanty occurrence of bioturbation and illuvial pedofeatures, and almost no presence of anthropogenic/organic constituents (Figure 3a–i). On the contrary, micromorphology of sample JH1 TS5 (Supplemental Materials

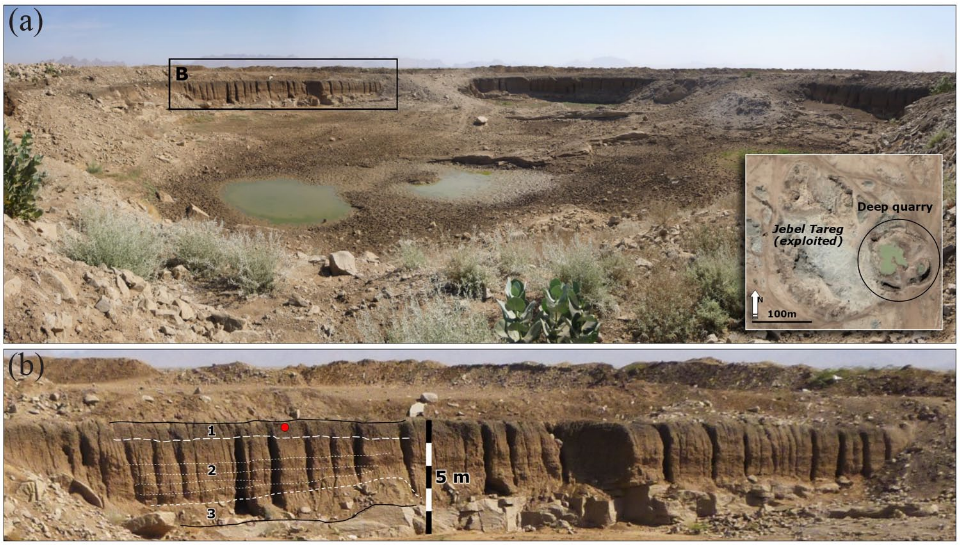

Figure 4. Jebel Tareg quarry – Site JT1. (a) East-facing overview of the quarry. Behind the observer lies the completely dismantled gneissic/granodioritic outcrop called Jebel Tareg. (b) Characterization of a portion of the exposed Quaternary pedostratigraphy. 1 indicates the Vertic Kastanozem-type soil, sampled for radiocarbon dating and micromorphological analyses (red dot 15.438659°N, 36.452548°E); 2 indicates the weathered ancestral alluvial deposit; 3 indicates gneissic saprolite (C horizon) sitting on the pristine crystalline basement. Atop the stratigraphy, unsorted disposal debris seals the sequence.

and Figure 3j–l), lifted a few metres downstream at a quote corresponding to B16, albeit revealing no substantial difference from sample JH1 TS4 in terms of C/F related distribution and microstructure, disclosed the presence of organic remains such as bone fragments, charcoal fragments and localized ash enrichment of the groundmass.

The upper surface of the stratigraphic sequence is sealed by a tight desert pavement composed of granodioritic clasts stabilized by a thin seasonal vegetation cover.

Archaeological remains from the gravel-enriched layer corresponding to sample B16 provided dating for the lowermost portion of the aeolian/colluvial deposit. Although the organic carbon yield of the layer did not reach measurability threshold for radiocarbon dating, the artefacts – mostly represented by ceramics fragments – belong unequivocally to the Middle and Classic/Late phases of the Gash Group culture (Manzo, 2019), therefore dating to the late third and early second mill. BCE. This means that almost the entirety of the aeolian/colluvial deposit is coeval or younger than the Gash Group, representing a perfectly fitting chronostratigraphic analogue with the palimpsest of the valley of Mahal Teglinos (Costanzo et al., 2022; Manzo, 2017; Swezey, 2001).

Jebel Tareg quarry – Site JT1

The gneiss quarry of Jebel Tareg is a commercial facility located a few hundred metres southeast of the city of Kassala, just east of the Jebel Taka (15.438268°N, 36.452442°E) (Figures 1 and 4a). The quarrying activity exposed a pre-Quaternary cover sitting directly on the underlying subhorizontal crystalline basement (Figure 4b). The Quaternary succession is composed of 4–6 m of unconsolidated to weakly consolidated layers: the deeper portion, which was not sampled, comprises several alternating bleached and iron-rich silty clay layers and horizons, likely related to ancestral fluvial deposition followed by hydromorphism and paedogenesis; the upper portion is a ~70 cm thick, laterally extensive dark organic horizon characterized by strongly expressed, very hard small and medium-sized (3–10 cm) equilateral plinths. The organic horizon is in turn covered and masked by a layer of unsorted debris, deriving from quarry soil disposal and several other infrastructural and agricultural works carried out in the surroundings.

The organic horizon was sampled ~30cm beneath the upper surface for radiocarbon dating (sample JT20198/DSH9576_HA) and micromorphological analyses. Radiocarbon dating yielded an age of 5802 ± 40 years BP (6730-6490 years cal BP, 2σ). Micromorphology (Supplemental Materials and Figure 5a–h) discloses a mature deposit, rich in small (~100μm) equilateral, subangular to subrounded quartz clasts, accompanied by less abundant same-sized feldspars and occasional larger granitoid clasts, all included with an open porphyric C/F-related distribution within a dense, massive dark brown clay matrix showing argillopedoturbation with incipient fragmentation into smaller plinths (1st order decimetric plinths split into second order centimetric chaotic angular polihedrons) and occasional bioturbation. Occasional $CaCO_3$ clasts, equilateral and well rounded, are also present; these may have been inherited as load features from older riverine systems or from eroded calcretes or Bk soil horizons that are still present in small, degraded patches in the outskirts of the larger inselbergs (Costanzo et al., 2022). The matrix shows widespread humus enrichment, widespread unaltered dendritic Fe/Mn nodules, oxide hypo-coating of the $CaCO_3$ clasts, and debris infilling of planar voids separating plinths. Such features, considering the radiocarbon dating ascribable to a wet period of the middle Holocene, are compatible with a polycyclic soil formation that started with the establishment, atop of the ancestral laterites, of a Kastanozem-type soil that formed under a warm prairie environment during a period of slightly higher water availability, followed by a transition to a Vertic Kastanozem-type soil promoted by rainfall hyper seasonality under a warm semi-arid climate (Eitel and Eberle, 2001; Eitel et al., 2002).

Jebel Maman – Site JM1

Jebel Maman is the name of a group of gold-bearing hills and inselbergs located at the very southern periphery of the Red Sea Hills, ~100km northeast of the city of Kassala (Figures 1 and 6a). The local assemblage of bedrock lithologies differ slightly from the other two locations, including metasedimentary hills – namely greenschists (GRAS, 2004) – along with gneiss basement

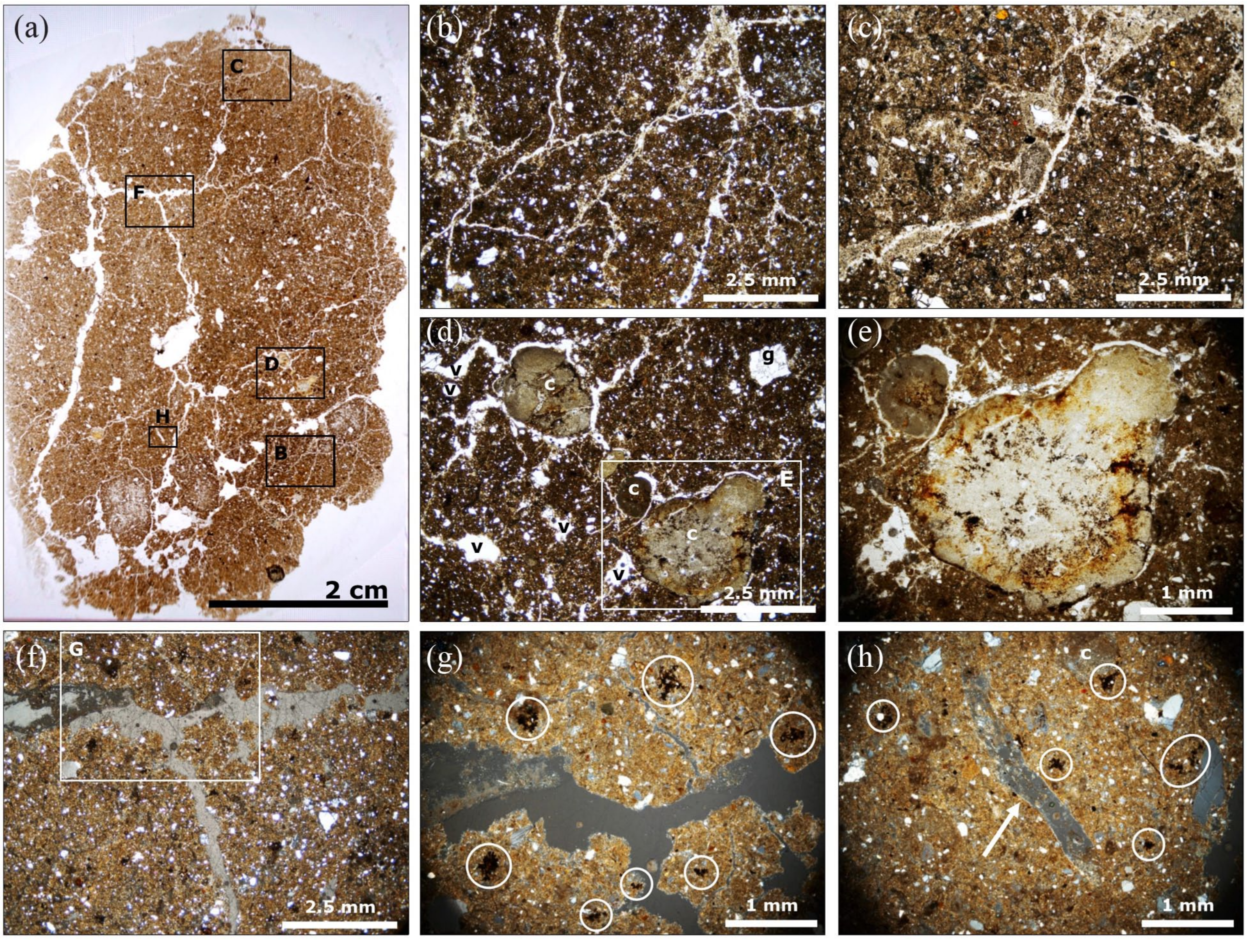

Figure 5. Selected thin section micrographs from Site JT1. (a) Scan of the soil thin section, highlighting the dark brown general colour coupled with well-expressed planar voids separating the mass in plinths and polyhedrons. (b and c) PPL micrographs highlighting the open porphyric C/F-related distribution and the presence of several thin incipient planar voids and vesicles and a general vertic structure. Small angular quartz clasts (bright white speckles) are dispersed within a fine silty clay brown matrix. (d and e) Well-rounded $CaCO_3$ clasts (c) show hypo-coating oxidation and growth of ferruginous nodules within their mass, suggesting they were already present within the deposit at the beginning of the paedogenesis. A small granite angular clast (g) is also visible in (d). Voids are indicated with (v). (f and g) XPL micrographs highlighting, again, the open porphyric C/F-related distribution and the presence of undisturbed dendritic and mamillated ferruginous nodules growing within the groundmass (white circles). The bright speckles in (f) are predominantly subangular to subrounded quartz grains, with lesser feldspar grains and occasional granitoid and mafic accessories. (h) Another example of dendritic and mamillated ferruginous nodules (white circles) growing within bioturbated (white arrow) groundmass, surrounded by small quartz grains arranged in open porphyric distribution within the matrix (XPL).

outcrops and granodioritic plutons. The Quaternary pediments and cover in the area are moderately more consolidated than in the area of Kassala, and covered with coarser angular debris forming a tight *hamada* surface (Knight and Zerboni, 2018). Nevertheless, the deposits are still subjected to pervasive gullying, although the depth and size of the gullies are smaller than those found, for example, around Jebel Haura. This may be due to the reduced thickness of the unconsolidated pediments, as well as the smaller dimensions of the rocky outcrops, which convey lesser rainwater over shorter altitude gradients, resulting in weaker and less disruptive flash floods. The extended area surrounding the site, being far from cities and stationary settlements that subsist with the agricultural land to the west of the Gash river's endorheic terminal fan, is not cultivated and receives lesser visitors, preserving a glimpse of the present day's potential natural landscape of the region, dominated by seasonal short-grass hot steppe stabilizing the unconsolidated substrate, and xerophyte tunnel vegetation flanking the ephemeral watercourses and *wadis*.

The section chosen for analysis is a 0.7 m spontaneous exposure of a very dark organic horizon covered and sealed by a 0.3 m thick paler silty layer (Figure 6b). The same stratigraphy is observed throughout the surroundings, suggesting an extended lateral continuity covering, at least, the lower land at the lobes of the coalescing pediments of the encircling hills. The lower dark horizon, dull grey in colour, is a mildly consolidated deposit forming small and brittle equilateral polyhedrons or weakly expressed small prisms, with no macroscopic archaeological, faunal, or botanical remains. The soil was radiocarbon dated (sample Beta-594956) to 6260 ± 30 years BP (7270-7020 years cal BP, 2σ). The upper layer, light brown in colour, is a massive, non-stratified unconsolidated fine deposit, again with no macroscopic archaeological, faunal, or botanical remains except for the roots of the live grass cover, which disrupt the already fragile aggregation making it impossible to collect undisturbed samples for thin section micromorphology. The sequence is topped by a loose discontinuous *hamada* surface composed of scatters of fine gravel.

Sedimentological analyses carried out on two bulk samples (Figure 6c), one for each layer/horizon, reveal a rather similar grain size distribution, dominated by aeolian fine sand and silt with almost no coarse sand and gravel content ($B1 = 0.53\%$, $B2 = 0.27\%$) and very limited amounts of clay as well. Conversely, analyses of the organic substance and $\%CaCO_3$ content yielded results that differed vastly between the two samples: the pale

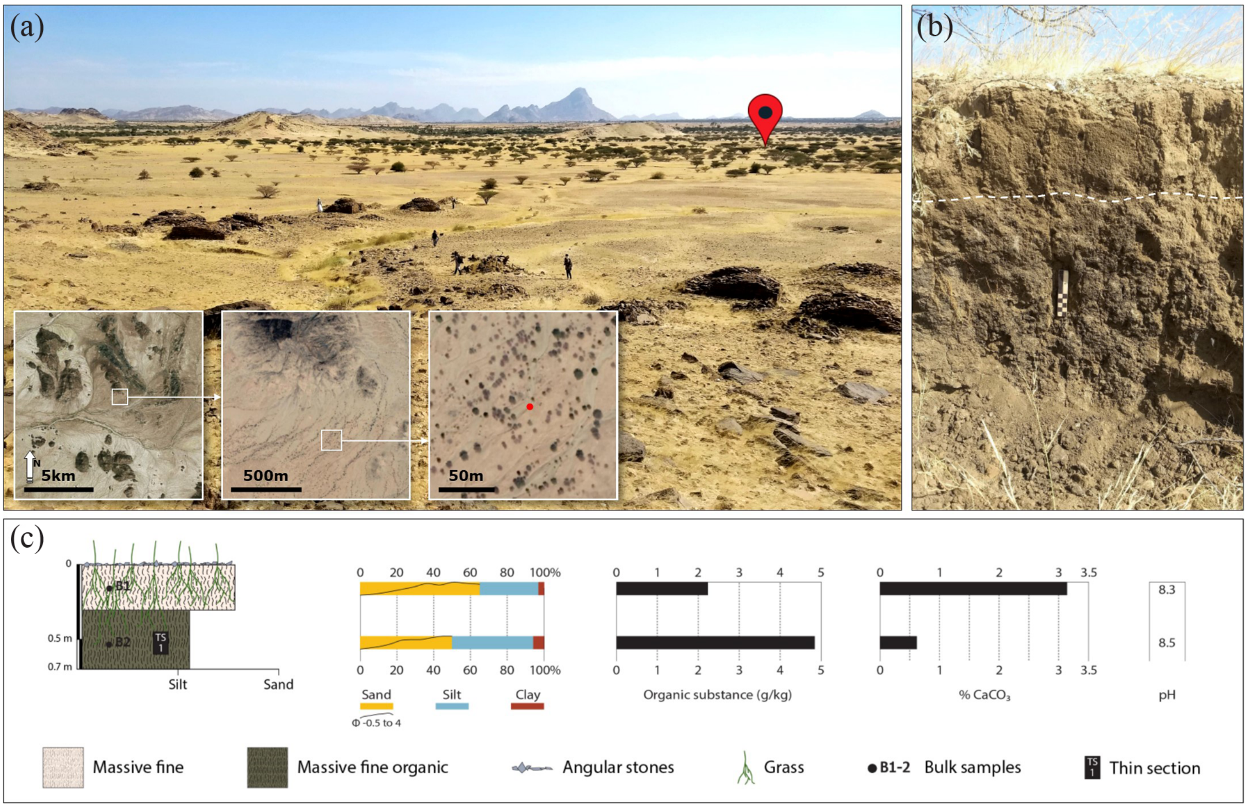

Figure 6. Jebel Maman Site JM1. (a) General settings of the site (16.279882°N, 36.836680°E), indicated by the red pinpoints in the south-facing panoramic photo and the smaller panel. The picture was taken in early December, when the ephemeral summer prairie has already dried up and only xerophytes and acacias survive on lower ground. In the foreground, the square stone structures are Medieval Islamic tombs called qubbas (Costanzo et al., 2021b). (b) Picture of the chosen section, cut by one on the countless small rills and gullies furrowing the inselberg's pediment. The dashed line separates the two main layers: pale brown sandy silt, sealing a dark grey organic horizon developed on silty sand. (c) Results of the pedosedimentary analyses carried out on the bulk samples gathered from the section. From left to right: stratigraphic log with samples, cumulative grain size distribution (gravel values for B1 and B2 are 0.53 and 0.27% respectively, not discernible from the cumulative histogram), organic substance content, $CaCO_3$ content, pH.

upper layer, although containing more organic substance compared with any of the sampled collected at Jebel Haura (Site JH1, Figure 2d), has less than half of that contained in the lower darker soil, which reaches just short of 0.5%. $CaCO_3$ content, on the other hand, shows an exactly opposite trend, with the upper layer being vastly richer in carbonate content ($B1 = 3.17\%$, $B2 = 0.62\%$).

Micromorphological analyses of the dark lower deposit (Supplemental Materials and Figure 7a–h) add details on the colour and internal structure of the soil. Similarly to Site JT1, rather than a uniform dark mass, the sample shows argillopedoturbation, with several chaotically arranged paler and darker patches, faintly plinthic or angular polyhedral in shape, of comparable coarse grain composition. These are differentiated by the aspect and composition of the groundmass, which is clay-like in the pale patches, and more fibrous in the dark ones. Pale and dark patches may be welded together (Figure 7d and g), or juxtaposed along thin planar voids (Figure 7f), or, again, gradually fading into each other (Figure 7a), and are all disrupted by bioturbation (Figure 7b, c and e). Rare amorphous $CaCO_3$ powdery concentrations, result of dissolution and rapid evapotranspiration, are found within the common structural voids and vesicles. Additionally, micromorphology offers a further insight on the source of the mineral fraction composing the parent material. In fact, the shape and weathering of the quartz clasts that compose most of the mineral fraction, paired with the analysis of the grain size distribution, indicates a loessic origin of the sediment (see Cremaschi et al., 2018). The soil's patchy colour and general spongy structure with faint angular aggregates, paired with the analytical results, suggest a relatively intense paedogenesis under a warm steppe environment with higher water availability than today, which led to isohumism (Duchaufour, 1982a) and the formation of a chernozem-type soil, again compatible with the loess substrate, with subsequently established moderate vertic properties prompted by the gradual decrease of rainfall in the last millennia.

Discussions

The stratigraphic, pedosentimentary and micromorphological analyses of the three selected sites, paired with the radiocarbon dating of significant contexts identified therein, provided noteworthy insights into the Holocene environmental evolution of the eastern portion of the Sudanese very outskirt of the Sahelian belt, at the transition between the alluvial plains of the Nile's basin and the Ethio-Eritrean Highlands. Therein, natural and anthropically enhanced surface erosional processes are causing a prominent fragmentation of an understudied Quaternary record (Costanzo et al., 2022). Even so, fragmentation was overcome by retrieving data from different natural archives that, when fitted together, define a model of Holocene paleoenvironmental evolution that is consistent and valid across the study region. In turn, results insert the region in the vast, yet still geographically discontinuous, archive of North African territories that are pivotal for the comprehension of Holocene human dynamics, and whose physiographic and paleoenvironmental study are key to a full awareness of processes of the human-environmental nexus.

The three study sites evidence the existence of several pedosedimentary features, whose formation was triggered by site-specific settings because of morphogenetic agents acting on different local topographies and pre-existing substrates. Nonetheless, their holistic examination shows a rather clear picture of the processes,

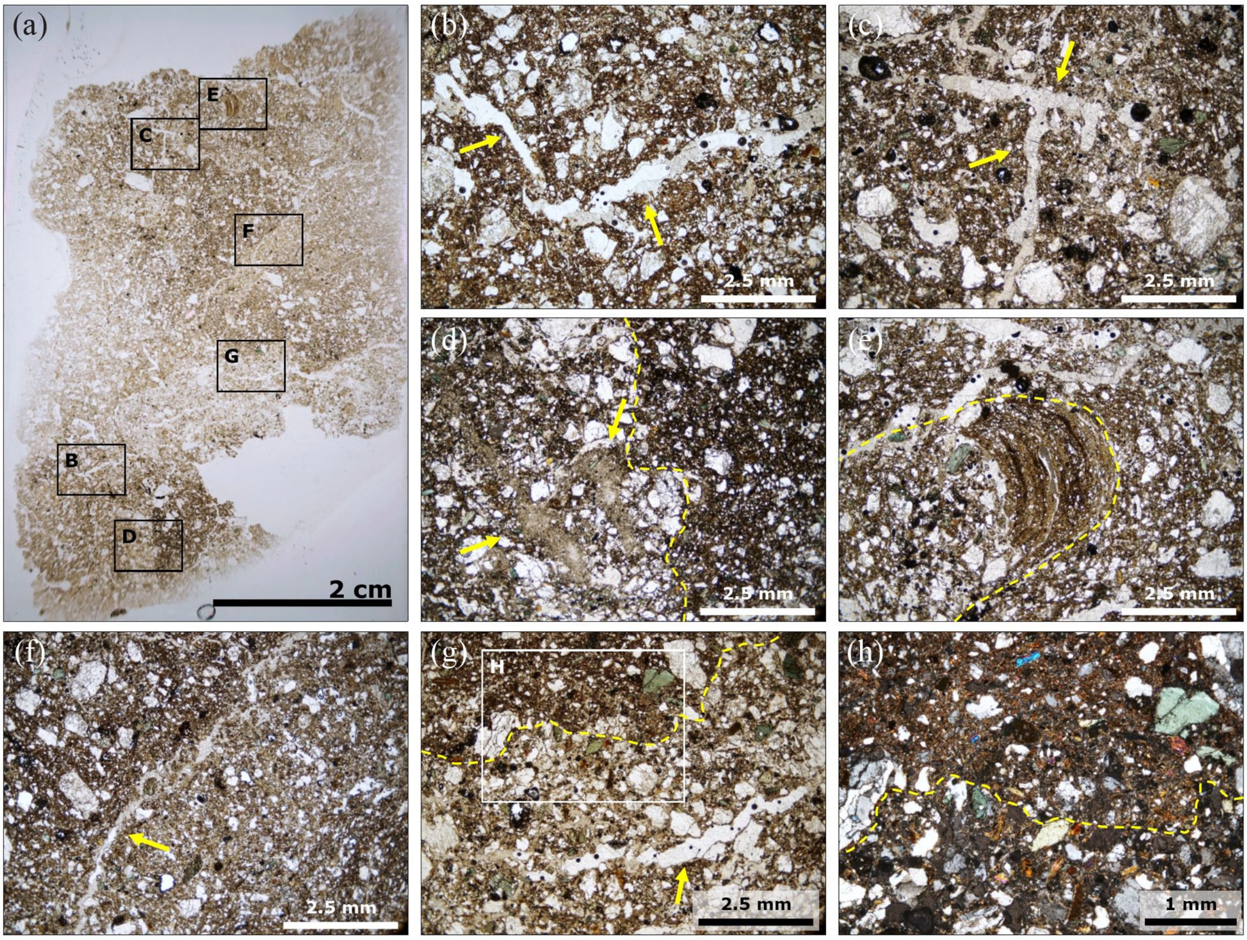

Figure 7. Selected thin section micrographs from Site JM1. (a) Scan of the soil thin section highlighting the general appearance of the soil mass, composed of paler and darker patches intimately and chaotically mixed. The boxes refer to the following panels. (b and c) Plane Polarized Light (PPL) and Cross Polarized Light (XPL) micrographs showing the general aspect of the sediment in dark patches, with subangular quartz sand dispersed into a fibrous spongy matrix disrupted by bioturbation (yellow arrows). (d) Pale and dark patches welded together (along the dashed line). The pale patch contains an amorphous $CaCO_3$ concretion (yellow arrows). The dark patch has a different textural composition than the pale one, with lesser and finer grained clasts dispersed within the matrix (PPL). (e) Detail of a large passage (bioturbation) feature (dashed line) (PPL). (f) Unwelded pale and dark patches, separated by a thin structural planar void. This time, the pale patch is finer grained than the darker one (PPL). (g and h) Welded pale and dark patches. This time the textural composition in similar. The yellow arrow indicates an incipient planar void originating from an unwelded pale/dark spot a few millimetres to the right (see panel a) (PPL and XPL).

climatic trends, and environmental transitions the happened in the region since the Early Holocene and up to present days (Figure 8).

Pre-Holocene

In two of the three locations, namely Site JT1 and Site JH1, ancestral deposits are found underlying the Holocene succession (Figure 8a). In Site JT1, quarrying activities exposed them down to the crystalline basement, revealing a thick succession of banded hydromorphic alluvial sediments. These were not studied in detail, but their deep desiccation, plinthic structure and general rusty colour suggest, at least, one or more phases of deep weathering (Duchaufour, 1982b) of the deposit. At Site JH1, just outside of the distal fringes of the pediment, satellite images and field survey revealed a reddened soil that represents the upper residual surface of the ancestral deposit, exposed subaerially as early as the first millennium CE as testified by archaeological scatters of grinding stones and ceramic bowls found in pristine position partially buried within very shallow pits (Manzo, 2019).

Early/middle Holocene

The most glaring feature from sites JT1 and JM1 is the preservation of buried isohumic soil horizons. In both cases, as proven by radiocarbon dates calibrated to 6730-6490 years BP (2σ) for JT1 and 7270-7020 years BP (2σ) for JM1, isohumic horizons formed in the Middle Holocene and are paedological remnants of environments that are no longer compatible with present-day climatic settings. In fact, they are referable to the Early/Middle Holocene phases of enhanced water availability that could sustain the prairie environments responsible for the formation of such deep and well-expressed organic profiles (Figure 8b). The same feature was observed in the well-studied valley of Mahal Teglinos (Costanzo et al., 2021a, 2022; Swezey, 2001), where a similar buried soil horizon was radiocarbon dated to 7430-7260 cal BP (2σ). The prairie environment model is further supported by the faunal assemblages from the Amm Adam archaeological sites (seventh–sixth mill. BCE) of the Gash river's fossil alluvial plain, which comprise kobs, reedbucks, hippos and buffalos (Geraads, 1983), all water-dependent species. Although the lateral extension of each patch of isohumic soil is not yet known, it is safe to assume that they may extend continuously interrupted by large rocky outcrops, only being truncated by active natural erosional processes or extensive modern cultivation (Costanzo et al., 2022).

At Site JM1, the isohumic soil is also associated with a peculiar parent material. In fact, as revealed by micromorphology and grain size distribution analysis, the fine-grained parent deposit appears to be of loessic origin (Yaalon, 1987). Further analyses shall be carried out in this respect, because this would represent a newly found sink location of peri-desert loess deposition (Crouvi

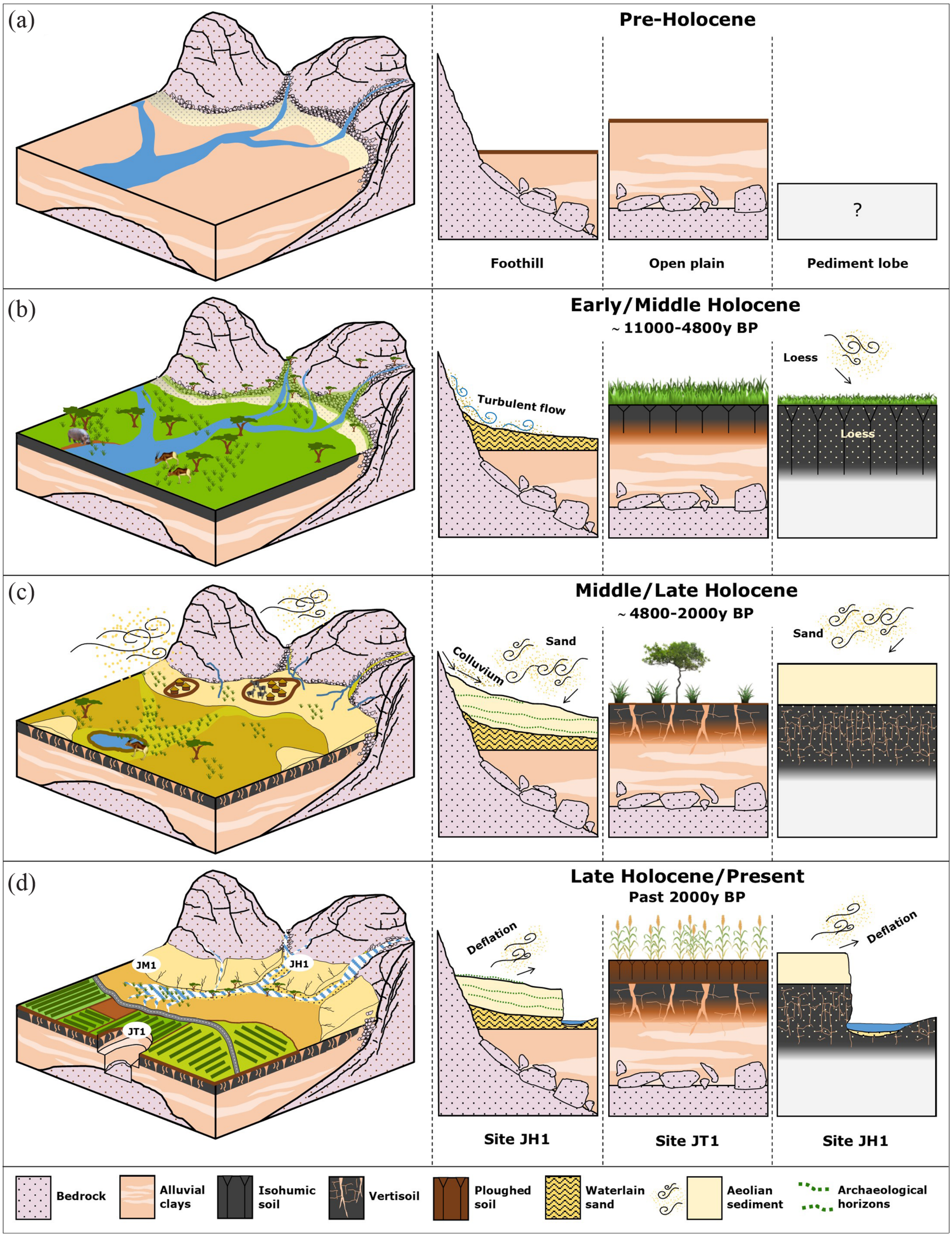

Figure 8. Theoretical model (not to scale) reconstructing morphogenetic processes and environments of the Kassala region, with site-specific pedostratigraphic sequences. (a) Pre-Holocene fluvial processes create the ancestral alluvial plain. No climatic and biotic data for this phase. (b) Warm-humid climate of the Early/Middle Holocene promote the formation of a prairie/woodland environment and the stabilization of foothills and open plain soil covers, with water-reliant faunal assemblages (Geraads, 1983; Manzo, 2017). (c) Drying climate of the Middle/Late-Holocene causes the vertisolization of the open plain's topsoil and the colluvial/aeolian accretion of the foothill pediments, engulfing coeval archaeological horizons. (d) Strong seasonal intermittent rains and intensive land exploitation disrupt the loose foothill deposits and mask the pristine landscape, causing the fragmentation of the archaeo-environmental record.

et al., 2010; Lancaster, 2020; Li et al., 2020; Smalley et al., 2019; Tsoar and Pye, 1987; Whalley et al., 1982), adding context to a much debated phenomenon that only has few and spread-apart case studies for Northern Africa (Coudé-Gaussen, 1990; Coudé-Gaussen and Rognon, 1988; Stokes and Horrocks, 2020). Interestingly, case studies of great similarity are found at the same latitudes in the southern Arabian Peninsula, where desert loess has been documented at the northern slopes of the Dhofar

Mountains in the Sultanate of Oman (Cremaschi and Negrino, 2005; Cremaschi et al., 2015), at Ras Al Khaimah in the United Arab Emirates (Goudie et al., 2000), and in the area of Sana'a in Yemen (Nettleton and Chadwick, 1996), where the loess sequence also promoted the formation of isohumic soil with a radiocarbon age very similar to the one measured for JM1 and then buried in the Late-Holocene.

While at Sites JT1 and JM1 water availability and topographic settings were promoting the maturation of stable organic soils, at Site JH1 the topography of the overlying bornhardts was causing the formation of chaotic thick sand-dominated deposits created by turbulent water discharge. Likely, the kinetic energy of the discharge and the quick sediment turnover was the primary cause for the lack of diffuse paedogenesis therein.

Middle – Late Holocene transition

Both isohumic soils from JT1 and JM1, together with the one from Mahal Teglinos, show secondary vertic properties that testify the climatic transition towards aridity that took place after the humid Middle Holocene. In fact, shrink-swell cycles of the groundmass, which are the primary cause of argillopedoturbation, are better expressed in a climatic regime of alternating wet and dry seasons. It is known that Middle Holocene's enhanced water availability, even though with still-debated timing and severity, eventually came to a halt (DeMenocal and Tierney, 2012; Shanahan et al., 2015), leading north Africa into a different climatic regime, which in turn promoted a new set of surface processes different from those acting in the previous several millennia.

For the Kassala region, this mainly meant aeolian deflation of open plains, with associated aeolian accretion of the pediments surrounding the large inselbergs that constitute wind breaks becoming dust traps (Figure 8c) (Middleton, 1985). This is particularly evident at Site JH1, where aeolian quartz and biotite dust contributed to the formation of the 2.5 m thick massive deposit sitting above the water-lain sands. Crucially, dust deposition is accompanied by equally present colluvial intake, that is, granitoid and granodioritic sand and gravel chaotically mixed with the fine aeolian sediment. Because in the entire deposit only four well-distinguishable gravel-enriched layers are found, it is reasonable to consider the aeolian and colluvial processes to be acting with equal intensity in tight alternance. This alternance, rather than leading to the formation of a manifestly layered deposit, promoted the growth of a chaotic admixture driven by gravitative redistribution during mild water-led colluvial events. In truth, the four gravel-enriched layers are associated with Gash Group archaeological remains or peaks of organic substance (Figure 2d), meaning that they formed during periods of relative stasis of the aeolian accretion possibly associated with transient humid episodes. In general, the stratigraphy of site JH1 is the result of aeolian-led processes in hot semi-arid climate and a local environment characterized by short ephemeral grasses, which protracted for ~2000 years between the end of the Middle Holocene's humid conditions and the onset of later climatic settings that underlie the origin of the widespread gullying affecting the region's pediplains. Substantiation for the hypothesis of the hot steppe environment comes from the faunal assemblages of Mahal Teglinos (Gautier and Van Neer, 2006; Manzo, 2017), namely from Gash Group and Mokram Group archaeological strata (mid-third – early first mill BCE), which comprise, along with domesticated bovids and ovicaprines, buffalos from the inundated Gash river, and gazelles and dikdiks from the drying up eastern open plains.

The top layer from site JM1 is, again, an aeolian fine-sand deposit. Micromorphology for this layer is missing, but the massive sedimentary structure of the deposit, the almost total lack of gravel and coarse sand, and its markedly centre/right skewed grain size distribution is compatible, as for the underlying horizon, with wind-driven processes. If observed from a wider regional perspective, and considering the $CaCO_3$ concentration measured in the sample (Figure 6c), its formation may be explained as a result of a twofold condition: (i) scarce colluvial intake caused by lesser seasonal rainfall compared to the southern locations (Figure 1) and by the relatively lower gradient and greater distance of the overlying inselberg's hillslope, and (ii) the presence, ~150 km northeast, of a vast source area of wind-blown sand and limestone dust that is the dried up dune-interdune basin system of the Middle Pleistocene Atbara Paleolake (Abbate et al., 2010). By extension, due to the consistency of the region-al's physiography (Costanzo et al., 2021a), every rocky spur of the northern hinterland of Kassala could meet the criteria to be a peri-desert loess sink for dust intake coming from neighbouring source locations, therefore representing potential high-resolution palaeoclimatic and paleoenvironmental archives especially if hosting buried soil horizons as in the case of Site JM1.

Late-Holocene and present days

A subsequent climatic transition is not registered in accretional sedimentary record, but rather in the loss of it (Figure 8d). In fact, the pervasive gullying that exposed the very sections considered in this research, is the result of a shift from the stable aridity of the Middle to Late-Holocene transition to hyper seasonality, characterized by dry spells alternating with increasingly powerful and disruptive flash floods that taint the pristine unconsolidated deposits, especially the pediments encircling the inselbergs. As emerged from the in-depth study of the valley of Mahal Teglinos (Costanzo et al., 2022), whose environmental and archaeological records are particularly rich and well-preserved, and from other studies from localities of adjacent regional contexts (Mawson and Williams, 1984; Williams and Nottage, 2006), such shift happened supra-regionally somewhen around the middle/late first millennium BCE. Nevertheless, the geomorphological outcome that can be observed today cannot be attributed solely to climate and rainfall dynamics. In fact, deeper causes related to the regional human-environmental nexus and new emerging subsistence economies underlie the feedback looping morphogenetic processes that are, still to present-day, responsible for soil loss and erosion in the region. By the mid-first millennium BCE, the regional economy downsized due to supra-regional shifting power balances, and large settlements such as Mahal Teglinos and JH1 were abandoned. Pastoralism became widespread across the land with seasonal camps and flocks of ovicaprines (Manzo, 2017), and zoogeomorphological processes were triggered as the delicate *hamada* surfaces, which offer protection to the summit of the unconsolidated pedostratigraphies such as that of Site JH1, were stripped by trampling and grazing, exposing weakened surfaces to the action of splashing raindrops and hillside channelled water, which started eroding the ground creating, in turn, more erodible surface (Zerboni and Nicoll, 2019). Still to present days, with an even increasing intensity of the summer monsoon caused by a contracting relapse period unmatched by the total rainfall yield, which remains unvaried (Hulme and Tosdevin, 1989; Zhang et al., 2012), zoogeomorphologically and anthropogenically enhanced processes acting on the delicate pediments are in place. Intensive agriculture eroded and masked the natural archives across very large areas, and vehicles and large flocks move from the exhausted harvested crops to unmanaged grassy raised ground in search of food resources year-round, causing instability and ultimately irreversible loss and fragmentation of archaeo-environmental archives.

In general, isohumic soils, typical of warm prairie/open savanna environments, are commonly found and date radiometrically to the Middle Holocene, adding new land to the records of present-day North African arid regions that used to host wetter habitats. The isohumic soils, in turn, are buried under a sedimentary cover, deposited between the late-third and mid-first millennia BCE, composed of unconsolidated fine-grained sands, silts, and gravel. This is especially true nearby tall granitoid inselbergs, which act both as topographic traps for wind-blown dust and source for colluvial gravel. Therein, unconsolidated pediment deposits can reach a thickness of a few metres, encasing archaeological strata and archiving short-term compositional variations that are diagnostic for morphogenetic processes at the local scale but, again, are consistent between sites that are far apart. Regional consistency is found for late and contemporary Holocene erosional processes as well. These are driven by a conjunction of hyper seasonal climate and zoogeomorphologically and anthropogenically enhanced processes, that have been causing pervasive gullying and soil destabilization since the mid-first millennium BCE.

Conclusions

Geomorphological, pedosedimentological, and micromorphological analyses, and archaeological and radiometric dating, were carried out on three naturally exposed sections from different, spread-apart locations of the eastern portion of the Kassala region of Sudan, close to the Eritrean border at the interface between the easternmost reaches of the Nile basin's alluvial plains and the Ethio-Eritrean Highlands. Our results disclosed the multiple steps of environmental evolution of the area. The region is characterized by the presence of a vast polygenic pediplain, that is the ultimate result of the dismantling of the regional gneiss crystalline basement and granodioritic plutons still emerging from the plain as inselbergs in the form of tall bornhardts assemblages. The three sites here investigated were found bearing fragmentary pedosedimentary and paleoenvironmental archives because of complex site-specific morphogenetic palimpsests and present-day zooanthropogenically-enhanced erosion. Yet, the combined analytical outcomes of the three sites, together with substantiation from the previously known site of Mahal Teglinos and the study of faunal assemblages from archaeological contexts of the area, provides a composite, regionally consistent picture of the Holocene pedosedimentary processes and paleoenvironmental evolution. Isohumic soils dating to the sixth–fifth millennia BCE are found across the region, developing on pre-existent substrates that vary depending on latitude and topographic settings. Most notably, in one location the isohumic soil presents chernozem-like characteristics and is found on a coeval thickening body of peri-desert loess. The isohumic soils are remnants of warm prairie/open savanna environments of the Middle Holocene, when early human communities would have settled in seminomadic hunting-foraging groups relying on water-dependent game and plant species. Meanwhile, at the steep foothills of larger inselbergs, turbulent water discharge would create sandy/gravelly pediments merging gradually into the grassy plain.

The isohumic soils and the water-lain sandy gravels were later buried by loose aeolian dust and hillslope colluvium deposited during the arid climatic transition of the Middle/Late-Holocene. Again, the thickness and characteristics of the aeolian/colluvial deposits are location-specific; they may be almost non-existent, or reach metric thickness in correspondence of the foothill of tall rocky inselbergs acting as dust traps and source of colluvium during composite morphogenetic processes driven by alternating dry and wet spells.

All the deposits are currently cut and disrupted by pervasive gully erosion, which is the late-stage result of the Holocene human-environmental nexus: flash flood-driven soil loss is enhanced by zoogeomorphological and anthropogenic disruption of the delicate surface of unconsolidated deposits, which are subject to feedbacking mechanisms that are causing large areas to be eroded and washed downstream, losing archaeological record as well. Although the erosional process has been in place for more than two millennia, urbanization and intensive agriculture enforced only in the last few decades have been paramount in exacerbating the irreversible damage.

The results of this study offer several hints upon the ideal course of action in paleoenvironmental and archaeological research. On one hand they show how, for novel research endeavours, obtaining data over extensive areas, rather than intensive insight on a single isolated site, provides a baseline for future reference and a clear picture of the potential of a region under diverse points of view. Integrating well-established archaeological knowledge with radiometric anchorage of pivotal pedostratigraphic newly found contexts, creates new and fundamental data on the areal extension of paleoenvironmental trends and phenomena and, most crucially, raises awareness on extant widespread morphogenetic processes that need be addressed for the institution of sustainability policies. On the other hand, hints emerged on the importance of Late Quaternary pedosedimentary palimpsests in marginal (and understudied) areas that lack remarkable high-resolution archives (Forti et al., 2023; Nicoll and Murphy, 2014). Pedosedimentary palimpsest are, for their nature, complex bodies of sediment characterized by phases of accretion and erosion that may carry low temporal resolution and high areal fragmentation. By considering every feature of the natural landscape as a potential missing link in the reconstruction of its complete paleoenvironmental history, low temporal resolution and areal fragmentation are overcome by cross-referencing. Hence, accurate interpretations of the complex succession of regional morphogenetic processes and climatic trends are obtained and can subsequently be inserted into supra-regional and continental dynamics.

Acknowledgements

We wish to thank the archaeological authorities of the Republic of the Sudan, the National Corporation for Antiquities and Museums, the Ministry division in Kassala and their welcoming staff. Part of this research was supported by the Italian Ministry of Education, Universities, and Research (MIUR) through the project 'Dipartimenti di Eccellenza 2018–2022' (WP4 – Risorse del Patrimonio Culturale) awarded to the Dipartimento di Scienze della Terra 'A. Desio' of the Università degli Studi di Milano.

Funding

The author(s) disclosed receipt of the following financial support for the research, authorship, and/or publication of this article: This research was carried out within the frame of the IAEES – Italian Archaeological Expedition to the Eastern Sudan (University of Naples 'L'Orientale'), funded by the Università di Napoli 'L'Orientale', ISMEO-Associazione Internazionale di Studi sul Mediterraneo e l'Oriente, and the Italian Ministry of Foreign Affairs. The Expedition is also generously supported by the Regional Government of the Kassala State.

ORCID iD

Stefano Costanzo https://orcid.org/0000-0002-0269-075X

Supplemental material

Supplemental material for this article is available online.

References

Abbate E, Albianelli A, Awad A et al. (2010) Pleistocene environments and human presence in the middle Atbara valley (Khashm el Girba, eastern Sudan). *Palaeogeography Palaeoclimatology Palaeoecology* 292(1-2): 12–34.

Beck HE, Zimmermann NE, McVicar TR et al. (2018) Present and future Köppen-Geiger climate classification maps at 1-km resolution. *Scientific Data* 5: 180214.

Beldados A, Manzo A, Murphy C et al. (2018) Evidence of sorghum cultivation and possible pearl millet in the second millennium BC at Kassala, eastern Sudan: Progress in African

Archaeobotany. In: Mercuri AM, D'Andrea AC, Fornaciari R et al. (eds) *Plants and People in the African Past*. Berlin: Springer International Publishing, pp.503–528.

Brass M (2018) Early North African Cattle Domestication and Its Ecological Setting: A Reassessment. *Journal of World Prehistory* 31: 81–115.

Bristow CS, Holmes JA, Mattey D et al. (2018) A late holocene palaeoenvironmental ‘snapshot’ of the Angamma delta, Lake Megachad at the end of the African humid period. *Quaternary Science Reviews* 202: 182–196.

Butzer KW (1959) Contributions to the Pleistocene geology of the Nile Valley. *Erdkunde*, 46-67. https://www.jstor.org/stable/23218435

Butzer KW (1960) Archeology and geology in Ancient Egypt: Geomorphological analysis permits reconstruction of the geography of prehistoric settlement. *Science* 132(3440): 1617–1624.

Butzer KW (1980) Pleistocene history of the Nile valley in Egypt and lower Nubia. *The Sahara and the Nile*, pp.253–280. Available at: http://sites.utexas.edu/butzer/files/2017/07/Butzer-1979-PleistoceneHistoryLowerNubia.pdf.

Butzer KW (1982) *Archaeology as human ecology: method and theory for a contextual approach*. Cambridge: Cambridge University Press.

Caton-Thompson G and Gardner EW (1932) The prehistoric geography of Kharga Oasis. *Geographical Journal* 80(5): 369–406.

Clarke J, Brooks N, Banning EB et al. (2016) Climatic changes and social transformations in the near East and North Africa during the ‘long’ 4th millennium BC: A comparative study of environmental and archaeological evidence. *Quaternary Science Reviews* 136: 96–121.

Costanzo S, Zerboni A, Cremaschi M et al. (2021a) Geomorphology and (palaeo-)hydrography of the Southern Atbai plain and western Eritrean Highlands (Eastern Sudan/western Eritrea). *Journal of Maps* 17(2): 51–62.

Costanzo S, Brandolini F, Idriss Ahmed H et al. (2021b) Creating the funerary landscape of eastern Sudan. *PLoS One* 16(7): e0253511.

Costanzo S, Zerboni A and Manzo A (2022) Active surface processes at Mahal Teglinos (Kassala, eastern Sudan): Archaeological implications for an endangered protohistoric site in Sahelian Africa. *Journal of Archaeological Science Reports* 43(6456): 103452.

Coudé-Gaussen G (1990) The loess and loess-like deposits along the sides of the western Mediterranean Sea: genetic and palaeoclimatic significance. *Quaternary International* 5: 1–8.

Coudé-Gaussen G and Rognon P (1988) The Upper Pleistocene loess of southern Tunisia: a statement. *Earth Surface Processes and Landforms* 13(2): 137–151.

Cremaschi M and Negrino F (2005) Evidence for an abrupt climatic change at 870014C yr B.P. In rockshelters and caves of Gebel Qara (Dhofar-Oman): Palaeoenvironmental implications. *Geoarchaeology* 20(6): 559–579.

Cremaschi M, Trombino L and Zerboni A (2018) Palaeosoils and relict soils: A systematic review. In: Stoops G, Marcelino V and Mees F (eds) *Interpretation of Micromorphological Features of Soils and Regoliths*. Amsterdam: Elsevier, pp.863–894.

Cremaschi M, Zerboni A, Charpentier V et al. (2015) Early–Middle Holocene environmental changes and pre-Neolithic human occupations as recorded in the cavities of Jebel Qara (Dhofar, southern Sultanate of Oman). *Quaternary International* 382: 264–276.

Cremaschi M, Zerboni A, Mercuri AM et al. (2014) Takarkori rock shelter (SW Libya): An archive of Holocene climate and environmental changes in the central Sahara. *Quaternary Science Reviews* 101: 36–60.

Cremaschi M, Zerboni A, Spötl C et al. (2010) The calcareous tufa in the Tadrart Acacus Mt. (SW Fezzan, Libya): an early Holocene palaeoclimate archive in the central Sahara. *Palaeogeography Palaeoclimatology Palaeoecology* 287(1-4): 81–94.

Crouvi O, Amit R, Enzel Y et al. (2010) Active sand seas and the formation of desert loess. *Quaternary Science Reviews* 29(17-18): 2087–2098.

Crowfoot JW (1922) A note on the date of the towers. *Sudan Notes and Records* 5: 83–87.

DeMenocal PB and Tierney JE (2012) Green Sahara: African humid periods paced by Earth's orbital changes. *Nature Education Knowledge* 3(10): 12.

Duchaufour P (1982a) Soils with matured humus: Isohumic soils and vertisols. In: Duchaufour P (ed) Pedology: Pedogenesis and classification. Dordrecht: Springer, pp.236–269.

Duchaufour P (1982b) Sesquioxide-rich soils. In: Duchaufour P (ed) *Pedology*: Pedogenesis and classification. Dordrecht: Springer, pp.373–425.

Eitel B and Eberle J (2001) Kastanozems in the Otjiwarongo Region (Namibia): Pedogenesis, associated soils, evidence for landscape degradation. *Erdkunde* 55: 21–31.

Eitel B, Eberle J and Kuhn R (2002) Holocene environmental change in the Otjiwarongo thornbush savanna (Northern Namibia): Evidence from soils and sediments. *CATENA* 47(1): 43–62.

Elsadig SO (2000) The domed tombs of the eastern Sudan. *Sudan and Nubia* 4: 37–43.

Fattovich R, Sadr K and Vitagliano S (1988) Society and territory in the Gash delta (Kassala, eastern Sudan) 3000 BC-AD 300/400. *Origini Rivista di Prehistoria e Protostoria delle Civiltà Antiche* 14: 329–358.

Forti L, Costanzo S, Compostella C et al. (2023) The geoarchaeological investigation on the defunctionalisation of an Assyrian canals system reveals late-Holocene land use transitions in Northern Mesopotamia. *The Holocene* 33: 416–431.

Gale S and Hoare PG (2012) *Quaternary Sediments: Petrographic Methods for the Study of Unlithified Rocks*. Caldwell, NJ: Blackburn Press.

Gasse F (2000) Hydrological changes in the African tropics since the Last Glacial Maximum. *Quaternary Science Reviews* 19(1-5): 189–211.

Gatto MC and Zerboni A (2015) Holocene supra-regional environmental changes as trigger for major socio-cultural processes in northeastern Africa and the Sahara. *African Archaeological Review* 32: 301–333.

Gautier A and Van Neer W (2006) Animal remains from Mahal Teglinos (Kassala, Sudan) and the arrival of pastoralism in the southern Atbai. *Journal of African Archaeology* 4(2): 223–233.

Geological Research Authority of the Sudan (2004) Geological map of the Sudan 1:2.000.000. *Geo3 Institute for Geo Research, TFH Berlin*.

Geraads D (1983) Faunal remains from the Gash delta, Sudan. *Nyame Akuma* 23: 2.

Giancristofaro E (2021) Jebel Hawrā, a new archaeological site in eastern Sudan. *Sudan and Nubia* 25: 209–221.

Goudie AS, Parker AG, Bull PA et al. (2000) Desert loess in ras Al Khaimah, United Arab Emirates. *Journal of Arid Environments* 46(2): 123–135.

Heiri O, Lotter AF and Lemcke G (2001) Loss on ignition as a method for estimating organic and carbonate content in sediments: Reproducibility and comparability of results. *Journal of Paleolimnology* 25(1): 101–110.

Heitz C, Laabs J, Hinz M et al. (2021) Collapse and resilience in prehistoric archaeology: Questioning Concepts and causalities in models of climate-induced societal transformations. In: Erdkamp P, Manning JG and Verboven K (eds) *Climate Change and Ancient Societies in Europe and the Near East. Palgrave Studies in Ancient Economies*. Cham: Palgrave Macmillan, pp.127–129.

Hulme M and Tosdevin N (1989) The tropical easterly jet and Sudan rainfall: A review. *Theoretical and Applied Climatology* 39: 179–187.

Jaouadi S, Lebreton V, Bout-Roumazeilles V et al. (2016) Environmental changes, climate and anthropogenic impact in south-east Tunisia during the last 8 kyr. *Climate of the Past* 12(6): 1339–1359.

Johnson PR, Andresen A, Collins AS et al. (2011) Late Cryogenian–Ediacaran history of the Arabian–Nubian shield: A review of depositional, plutonic, structural, and tectonic events in the closing stages of the northern east African Orogen. *Journal of African Earth Sciences* 61(3): 167–232.

Knight J and Zerboni A (2018) Formation of desert pavements and the interpretation of lithic-strewn landscapes of the central Sahara. *Journal of Arid Environments* 153: 39–51. DOI: 10.1016/j.jaridenv.2018.01.007

Lancaster N (2020) On the formation of desert loess. *Quaternary Research* 96: 105–122.

Li Y, Shi W, Aydin A et al. (2020) Loess genesis and worldwide distribution. *Earth-Science Reviews* 201: 201–102947. DOI: 10.1016/j.earscirev.2019.102947

López-García JM, Agustí J and Aouraghe H (2013) The small mammals from the Holocene site of Guenfouda (Jerada, Eastern Morocco): chronological and paleoecological implications. *Historical Biology* 25(1): 51–57. DOI: 10.1080/08912963.2012.688198

Macphail RI and Goldberg P (2018) *Applied Soils and Micromorphology in Archaeology*. Cambridge: Cambridge University Press.

Manzo A (2017) *Eastern Sudan in Its Setting. The Archaeology of a Region Far From the Nile Valley*. Oxford: Archaeopress.

Manzo A (2019) Italian archaeological expedition to the eastern Sudan of the Università degli Studi di Napoli "l'Orientale" and ISMEO. Preliminary report of the 2019 field seasons. *Newsletter di Archeologia CISA* 10: 265–284.

Manzo A (2020) Back to Mahal Teglinos: New Pharaonic evidence from Eastern Sudan. *The Journal of Egyptian Archaeology* 106(1-2): 89–104.

Mawson R and Williams MAJ (1984) A wetter climate in eastern Sudan 2,000 years ago? *Nature* 309(5963): 49–51.

Mayewski PA, Rohling EE, Curt Stager J et al. (2004) Holocene climate variability. *Quaternary Research* 62(3): 243–255.

Mercuri AM, Clò E and Florenzano A (2022) Multiporate pollen of Poaceae as bioindicator of environmental stress: First Archaeobotanical evidence from the early–Middle Holocene site of Takarkori in the Central Sahara. *Quaternary* 5(4): 41.

Middleton NJ (1985) Effect of drought on dust production in the Sahel. *Nature* 316(6027): 431–434.

Murphy CP (1986) *Thin Section Preparation of Soils and Sediments*. Berkhamsted: AB Academic Publishers.

Nassr AH (2014) Large cutting tools variations of early Sudan Paleolithic from the site of Jebel Elgrian east of lower Atbara. *Der Antike Sudan. MittSAG* 25: 105–123.

Nettleton WD and Chadwick OA (1996) Late Quaternary, redeposited loess-soil developmental sequences, South Yemen. *Geoderma* 70(1): 21–36.

Nicoll K (2004) Recent environmental change and prehistoric human activity in Egypt and Northern Sudan. *Quaternary Science Reviews* 23(5-6): 561–580.

Nicoll K, Emmitt J, Kleindienst MR et al. (2021) Elinor Wight Gardner: Pioneer Geoarcheologist, Quaternary Scientist and Geomorphologist. *Geosciences* 11(7): 267.

Nicoll K and Murphy LR (2014) Soil and sediment archives of ancient landscapes, paleoenvironments, and archaeological site formation processes. *Quaternary International* 342: 1–4.

Nicosia C and Stoops G (2017) *Archaeological Soil and Sediment Micromorphology*. Hoboken: John Wiley & Sons.

Paul A (1952) Ancient Tombs in Kassala Province. *Sudan Notes and Records* 33: 54–57.

Reimer PJ (2020) Composition and consequences of the IntCal20 radiocarbon calibration curve. *Quaternary Research* 96: 22–27.

Ritchie JC and Haynes CV (1987) Holocene vegetation zonation in the eastern Sahara. *Nature* 330: 645–647.

Sandford KS (1929) The Pliocene and pleistocene deposits of Wadi Qena and of the Nile Valley between Luxor and Assiut (QAU). *Quarterly Journal of the Geological Society* 85(1-4): 493–548.

Shanahan TM, McKay NP, Hughen KA et al. (2015) The time-transgressive termination of the African humid period. *Nature Geoscience* 8: 140–144.

Shiner J (1971) The Prehistory and Geology of Northern Sudan, Part II. *Report to the National Science Foundation, Grant GS 1192*, Washington D.C.

Smalley I, Marshall J, Fitzsimmons K et al. (2019) Desert loess: A selection of relevant topics. *Geologos* 25: 91–102.

Stokes S and Horrocks J (2020) A reconnaissance survey of the linear dunes and loess plains of northwestern Nigeria: Granulometry and geochronology. In: Alsharhan AS, Glennie KW and Whittle GL (eds) *Quaternary Deserts and Climatic Change*. Boca Raton, FL: CRC Press, pp.165–174.

Stoops G (2021) *Guidelines for Analysis and Description of Soil and Regolith Thin Sections*, 2nd edn. Madison, WI: Soil Science Society of America Inc., Wiley.

Stoops G, Marcelino V and Mees F (2018) *Interpretation of Micromorphological Features of Soils and Regoliths*, 2nd edn. Amsterdam: Elsevier.

Swezey C (2001) Eolian sediment responses to late Quaternary climate changes: Temporal and spatial patterns in the Sahara. *Palaeogeography Palaeoclimatology Palaeoecology* 167: 119–155.

Tsoar H and Pye K (1987) Dust transport and the question of desert loess formation. *Sedimentology* 34(1): 139–153.

Walkley A and Black IA (1934) An examination of the Degtjareff method for determining soil organic matter, and a proposed modification of the chromic acid titration method. *Soil Science* 37(1): 29–38.

Whalley WB, Marshall JR and Smith BJ (1982) Origin of desert loess from some experimental observations. *Nature* 300(5891): 433–435.

Williams M and Nottage J (2006) Impact of extreme rainfall in the central Sudan during 1999 as a partial analogue for reconstructing early Holocene prehistoric environments. *Quaternary International* 150(1): 82–94.

Winchell F, Stevens CJ, Murphy C et al. (2017) Evidence for sorghum domestication in fourth millennium BC eastern Sudan: Spikelet morphology from ceramic impressions of the Butana Group. *Current Anthropology* 58(5): 673–683.

Wright DK (2017) Humans as agents in the termination of the African humid period. *Frontiers in Earth Science* 5. DOI: 10.3389/feart.2017.00004

Yaalon DH (1987) Saharan dust and desert loess: Effect on surrounding soils. *Journal of African Earth Sciences* 6(4): 569–571.

Zerboni A and Nicoll K (2019) Enhanced zoogeomorphological processes in North Africa in thehuman-impacted landscapes of the anthropocene. *Geomorphology* 331: 22–35.

Zhang Z, Xu CY, El-Tahir MEH et al. (2012) Spatial and temporal variation of precipitation in Sudan and their possible causes during 1948–2005. *Stochastic Environmental Research and Risk Assessment* 26: 429–441.